Max-Planck-Institut
für Meteorologie

REPORT No. 134

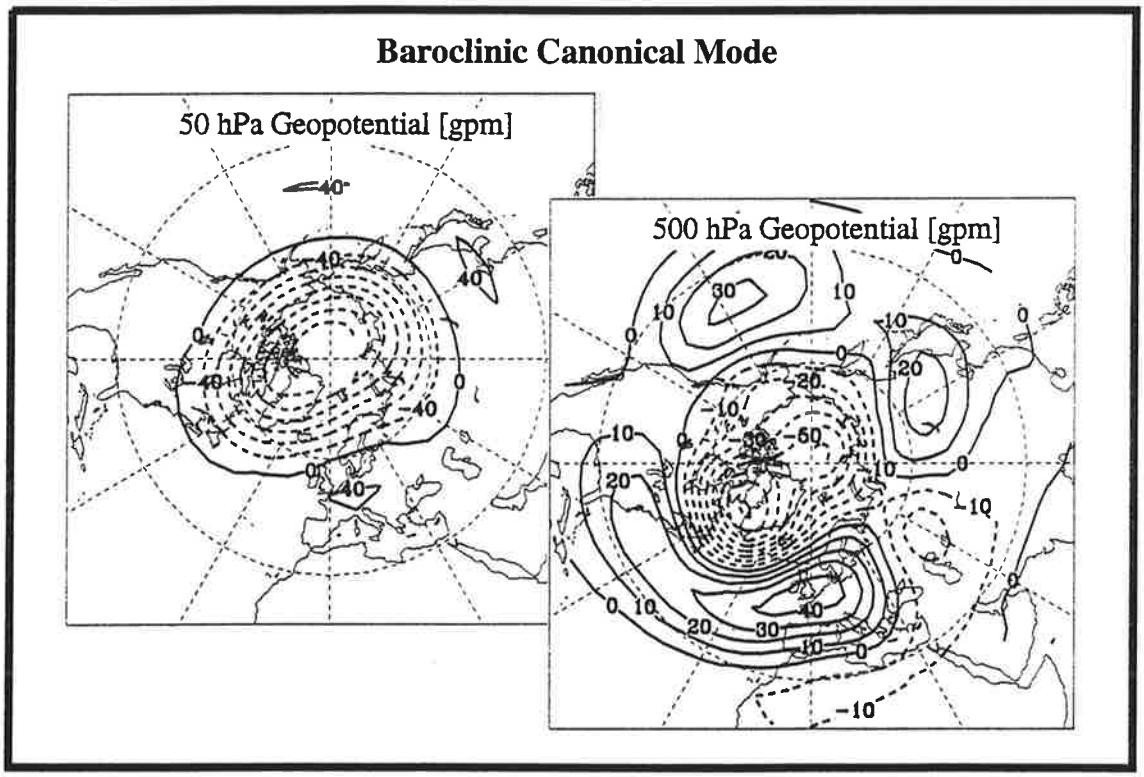

ON THE STATISTICAL CONNECTION BETWEEN TROPOSPHERIC AND STRATOSPHERIC CIRCULATION OF THE NORTHERN HEMISPHERE IN WINTER

by

JUDITH PERLWITZ · HANS-F. GRAF

HAMBURG, June 1994

AUTHORS:

Judith Perlwitz
Hans-F. Graf

Max-Planck-Institut
für Meteorologie

MAX-PLANCK-INSTITUT
FÜR METEOROLOGIE
BUNDESSTRASSE 55
D-20146 Hamburg
F.R. GERMANY

Tel.: +49-(0)40-4 11 73-0
Telefax: +49-(0)40-4 11 73-298
E-Mail: <name> @ dkrz.d400.de

ISSN 0937–1060

On the statistical connection between tropospheric and stratospheric circulation of the northern hemisphere in winter

Judith Perlwitz and Hans-F. Graf
Max Planck Institut für Meteorologie
Bundesstraße 55, D-20146 Hamburg, Germany
(submitted to Journal of Climate; June 2, 1994)

Abstract

The associated anomaly patterns of the stratospheric geopotential height field and the tropospheric geopotential and temperature height fields of the northern hemisphere are determined applying the Canonical Correlation Analysis (CCA). With this linear multivariate technique the coupled modes of variability of time series of two fields are isolated in the EOF space. The one data set is the 50 hPa geopotential field, the other set consists of different height fields of the tropospheric pressure levels (200 hPa, 500 hPa, 700 hPa, 850 hPa) and the temperature of the 850 hPa pressure level. For the winter months (December, January, February) two natural coupled modes, a barotropic and a baroclinic one, of linear relationship between stratospheric and tropospheric circulation are found. The baroclinic mode describes a connection between the strength of the stratospheric cyclonic winter vortex and the tropospheric circulation over the North Atlantic. The corresponding temperature pattern for an anomalously strong stratospheric cyclonic vortex is characterized by positive temperature anomalies over higher latitudes of Eurasia. These 'Winter Warmings' are observed e.g. after violent volcanic eruptions. The barotropic mode is characterized by a zonal wave number one in the lower stratosphere and by a PNA-like pattern in the troposphere. It was shown by Labitzke and van Loon (1987) that this mode can be enhanced e.g. by El Niños via the intensification of the Aleutian low.

ISSN 0937–1060

1. Introduction

In context with studies of the effect of volcanic eruptions on global climate (Graf et al., 1993a; Graf et al., 1993b; Kodera, 1993b), with solar-terrestrial relationships (Kodera and Yamazaki, 1990; Labitzke and van Loon, 1988) as well as with general circulation model (GCM) sensitivity studies (Boville, 1984) the interrelationship between stratospheric and tropospheric circulation was studied. These studies showed a possible impact of the strength of the stratospheric winter vortex, or the polar night jet (PNJ), on the structure of tropospheric planetary waves.

A possible mechanism by which stratospheric perturbations might cause significant alterations of the tropospheric circulation is suggested e.g. in Matsuno (1970) and Hines (1974). These ideas are confirmed by results of two-dimensional linear models describing stationary wave-propagation (Schmitz and Grieger, 1980; Geller and Alpert, 1980). They showed that changes of the stratospheric mean zonal wind influences the structure of the planetary waves and meridional heat flux in the troposphere. Tropospheric forced ultra-long vertically propagating planetary waves can be reflected at higher elevations, e.g. at the PNJ, and interfere constructively or destructively with the initial waves. Consequently, alterations of the reflection properties of the lower stratospheric zonal wind field, i.e. of the zonal mean wind speed, for vertically propagating planetary waves might change amplitudes and phases of the tropospheric planetary waves, and therefore change the tropospheric climate. In addition to the linear effects, Boville (1984) and Kodera et al. (1991) using GCMs driven by strengthened PNJ, showed some substantial non-linear effects on the stationary as well as on the transient wave behaviour.

Case studies for strong and weak PNJ winter months (Graf et al., 1993a; Kodera, 1993a) show good agreement between the results of linear models (Schmitz and Grieger, 1980) and observations for the middle tropospheric circulation. A considerable part of the effects therefore seems to result from the linear part of the stratosphere-troposphere interaction. The observations based on monthly data do not allow to judge whether the troposphere or the stratosphere is the leading element in the interaction. But the above mentioned model experiments all started out from a changed stratospheric circulation influencing the tropospheric climate.

The model studies allowed an explanation of the unexpected "Winter Warm-

ing" in higher latitudes of Eurasia found after strong tropical volcanic eruptions by e.g. Robock and Mao (1992) and Groisman (1992), which is the result of the enhancement of a natural circulation mode by differential heating of the tropical and polar stratosphere due to the absorption of long wave radiation at the volcanic aerosol (Graf et al., 1993b).

In our study, the Canonical Correlation Analysis (CCA) (e.g. Bretherton et al., 1992) is used to isolate the important coupled modes of variability between the time series of the fields of stratospheric and tropospheric circulation and temperature. The CCA is a multivariate statistical analysis technique exploring the linear association between two sets of variables. We use the CCA in the phase space of the Empirical Orthogonal Functions (EOF) (Barnett and Preisendorfer, 1987), in order to improve the signal to noise ratio. The used data sets are described in section 2, and the CCA is briefly outlined in section 3. A representation and discussion of the results follows in section 4, and conclusions are given in section 5.

2. Data

To study the stratospheric-tropospheric interaction, monthly averaged geopotential height and temperature data for different tropospheric and stratospheric pressure levels are used for the northern hemispheric region covering 20°N to the pole on a regular 5° x 5° grid. The tropospheric height fields of the 850 hPa, 700 hPa, 500 hPa and the 200 hPa level, and the 850 hPa temperature data are based on the analysis of the National Meteorological Centre (NMC). The 500 hPa time series covers winter months from 1957 through 1989, while the other series start only in 1962.

The 50 hPa height data were provided by the Stratospheric Research Group, F.U. Berlin. These data are produced from daily hemispheric analyses, mainly using radiosondes. The meridional resolution of the stratospheric grid is 10°. The grid interval is 10° longitude from 20°N to 70°N, and 20° longitude at 80°N. The pole point completes this grid, consisting of 235 grid points altogether.

3. Canonical Correlation Analysis

The theory of CCA was developed by Hotelling (1936). Since the 1960's this technique has become a preferred analysis method in empirical social science. In meteorology the CCA was introduced by Glahn (1968). Since the end of the

1980's, there have been a large number of applications, mostly in the field of climate diagnostics. Therefore, in this section only a short verbal description of the CCA follows. An exact derivation of the CCA is found e.g. in Anderson (1984).

As is mentioned in the introduction, with this technique it is possible to study the linear statistical association between two sets of variables in an optimized way. A coordinate transformation is performed in each phase space spanned by the two sets of variables, such that the correlation between the transformed sets of variables is maximized in pairs. The new transformed variables are called canonical variables, and the correlation coefficient of a pair of canonical variables is the canonical correlation coefficient. The pairs of canonical variables are ordered according to their canonical correlation coefficient. The pair with the maximum correlation is called the "first mode", the pair with the second highest value of the correlation coefficient is the "second mode", etc. The covariance between the original variables and their corresponding canonical variables is calculated to determine the structure of the canonical relationships.

This multivariate approach is especially useful when the interrelation between complex phenomena, not being describable with only few variables, is to be investigated. A calculation of a multitude of bivariate and multiple correlations leads to results which may underestimate the whole interrelation. In meteorological applications, the CCA is often used to study the connection between two space-time dependent variables (Barnett and Preisendorfer, 1987; Graham et al., 1987; Déqué and Servain, 1989; Metz, 1989; Wallace et al., 1992; Zorita et al., 1992; Barnston and Ropelewski, 1992). To study the connection between two fields of variables, the associated spatial anomaly pattern of the two fields (sometimes also called canonical correlation pattern) is determined by the calculation of the covariance between the original and the canonical fields of variables. Because the canonical variables are normalized to unity, the canonical correlation patterns represent the typical strength of the signal (Zorita et al., 1992). The canonical variables are time series of weights for the associated patterns which describe the strength and the sign of the patterns for each realization in time. The corresponding canonical correlation coefficient is an expression for the degree of the connection between the two fields represented by the respective canonical variables and the associated patterns. Together the canonical variables and canonical correlation patterns belonging to a canonical correlation coefficient define a coupled mode of the variability between the time series of the two data fields under consideration (Bretherton et al., 1992).

For meteorological applications the number of grid point variables is often less than the number of realizations in time and/or the spatial correlation between the variables of a data field is very high. This problem is mathematically soluble if each data field is orthogonalized by Principle Component Analysis (PCA). If then only those Principle Components (PCs) which explain a considerable part of the total variance are used for the CCA, the number of variables is reduced and a filtering of the data eliminating noise is achieved.

The mathematical description of the CCA on the basis of PCs is found in Barnett and Preisendorfer (1987). In Bretherton et al. (1992) and Barnston and Ropelewski (1992) vivid graphical representations about the technique are given. Since the number of meaningful EOFs, and with it the explained part of the total variance of the original variables, has to be chosen, this method is influenced by a subjective factor. If the number of temporal realizations is relatively small compared to the spatial degrees of freedom, the estimation of the EOFs is uncertain, and therefore, the results of the CCA are influenced by this subjectivity. Using a too large fraction of variance (near to 100%, i.e. poor filtering of the original time series) is associated with a large random error due to sampling errors. If too little variance is taken into account, it is possible that important information about the link of the two fields will be lost. Bretherton et al. (1992) suggested that a considered variance of about 70% to 80% is a good compromise between these two errors.

4. Results and Discussion

4.1. Approach and preprocessing

To investigate the interaction of stratospheric and tropospheric circulation, the canonical correlation of observed data of northern hemispheric geopotential heights are studied. With the CCA in the EOF space, the mean associated anomaly patterns of stratospheric and tropospheric height fields are determined in a filtered phase space. One basis set is the 50 hPa geopotential field, the other sets are different height fields of tropospheric pressure levels (200 hPa, 500 hPa, 700 hPa, 850 hPa). The results of a further analysis is given, where the same stratospheric set is used together with the temperature of the 850 hPa pressure level.

There are a number of methods to test the significance of the canonical correlation coefficient (Röhr, 1987). Their application requires knowledge of the

number of spatial degrees of freedom of the two fields. From the results of the PCA some conclusions about the number of degrees of freedom can be drawn. But the Empirical Orthogonal Functions are imperfectly estimated because the ratio of the number of realizations to the number of grid points is too small. This allows only a rough estimate of the number of degrees of freedom. For these reasons, the CCA is only used for the detection of the associated patterns. After the definition of the associated patterns, a local test of the found connections may be applied to the areas with highest explained variance in order to test the correlation coefficients with original data.

The investigation is concentrated on the winter months December, January, February, because for these months theoretical results from the literature (e.g. Charney and Drazin, 1961; Matsuno, 1970) allow us to expect the strongest coupling between the circulation of stratosphere and troposphere. The number of realizations is different for the individual analyses. It depends on the common available time period of the two sets of variables considered for a CCA. In each case as many realizations as possible are used. The long term means for each of the winter months and the corresponding anomalies are calculated at each grid point. Before executing the PCA, the anomalies are weighted with the square root of the cosine of the geographic latitude to consider the area represented by the grid points. In the figures however, this latitude weighting was not applied.

Labitzke and van Loon (1991) found that there exists a negative trend in the area weighted annual mean 50 hPa temperature of the northern hemisphere (10°N-90°N). Labitzke and van Loon (1994) investigated the lower stratospheric temperature trend in more detail. They showed the existence of a decadal oscillation (in conjunction with the sun spot cycle) overlaying a negative temperature trend. They also found a positive trend in the annual mean area weighted height of the pressure surface layers of the lower stratosphere. This indicates strong influence of tropospheric variations on the lower stratospheric pressure layers. In our study we find this trend to be positive in winter only south of 60°N. During winter (DJF) the 50 hPa layer height decreases with time from 60°N to the North Pole (Figure 1). This implies a strengthening of the PNJ due to the increased meridional temperature gradient near the polar circle.

The trends of the zonal mean of the height of the 50 hPa geopotential layer were computed for different latitudes. In Figure 1 for selected latitudes (30°N, 70°N) the time series are given together with the linear trend function (note that

the scale of the ordinate is larger north of the polar circle, because of the increased variability in this area). The t-test value for the linear regression coefficient describing the trend is given as well. With 36 degrees of freedom a t-test value of 2.03 determines the 95% significance threshold. The term trend here means a change of the mean value of the data with the time, tested against the noise. Thus, a 'significant trend' may also be part of a long-term oscillation of the climate etc. This, because of the shortness of the time series, cannot be tested. This means that the positive trends between 20°N and 40°N are statistically significant as well as the negative trend at 70°N. Between 50°N and 60°N the trend changes sign. In Figure 1c the height difference of the 50 hPa layer between 50°N and 60°N is displayed giving evidence of the statistically significant intensification of the PNJ.

A more detailed study of the geographical distribution and the possible origin of the trends is in preparation (Graf and Perlwitz, 1994). In our study we discuss the results based on the original time series. The computation of the canonical modes based on the detrended data does not show any remarkable difference.

4.2. EOFs of the 50 hPa height field

In this subsection a short description of the most important EOFs of the anomalies of the northern hemisphere 50 hPa field is given. These EOFs explain a large part of the variability of the data field, and the stratospheric part of the canonical patterns resulting from all the CCAs essentially follows these EOFs.

The first EOF and the corresponding standardized PC are shown in Figure 2a and Figure 3, respectively. The first EOF, explaining 52% of the total variance, describes the intensity of the cyclonic stratospheric vortex in winter. This can be proved by calculation of the correlation coefficient between the PC of the first EOF and the zonally averaged zonal component of the geostrophic wind. The mean of the geostrophic zonal wind component in 65°N at 50 hPa is very highly correlated with the first PC (r=-0.96). Thus, the time coefficients of the first EOF determine whether the stratospheric vortex is anomalously weak (positive coefficient) or anomalously strong (negative coefficient). Because the vortex is not really zonally symmetric, the first EOF and its PC contain some more information than does the zonal wind component alone.

The second and the third EOFs (Figure 2 b-c), explaining 14% and 8% of the

total variance, respectively, are very similar to a planetary wave of the zonal wave number one, but the second EOF is superimposed by a wave number two. With these three EOFs, which by definition are orthogonal, it is possible to explain a large part (74%) of the observed variability of the monthly averaged stratospheric height field in the northern hemisphere winter. These EOFs characterize the strength of the vortex and its disturbance by waves of wave number one and two.

The tropospheric EOFs will not be discussed here in detail, because these can be estimated only roughly. The smaller scale phenomena occurring in the troposphere lead to a smoother distribution of explained variance over the EOFs than was found in the stratosphere. In Figure 4 the variance, explained by the EOF of the 500 hPa layer is shown together with the estimated error (North et al., 1982; Fraedrich, 1986) of the explained variance. This makes clear that the EOFs cannot be separated adequately. Obviously the ratio between the spatial degrees of freedom and the number of realizations is much too small in the troposphere.

4.3. Results of the CCA

4.3.1. Geopotential

In the following, the results of the Canonical Correlation Analysis will be discussed. We concentrate on the results based on the EOFs describing about 75% of the total variance for both fields. This corresponds to 3 EOFs for the 50 hPa field and 8 to 9 EOFs for the tropospheric height fields. The canonical modes found are stable also if more variance is taken into account (for instance 90% of the total variance for both the tropospheric and stratospheric fields).

The study was performed for the 850, 700, 500 and 200 hPa layers. We shall concentrate here on the 500 hPa layer results since the time series are longest for this layer. For this analysis the months of the winters 1957/58 to 1988/89 (96 realizations) are used. The canonical correlation patterns of the three modes of the 50 hPa height essentially follow the first three EOFs. The pair of patterns of the first mode (Figure 5) explain 48% (12%) of the total variance of the 50 hPa (500 hPa) geopotential height field. Figure 6 shows the local variance at the individual grid points explained by the corresponding first canonical variables in our time interval. For the sake of clarity, in the Figure 6 the isolines of explained local variance of less than 20 % are omitted. Whereas the first canonical correlation pattern of the stratospheric field describes a global scale signal, the tropo-

spheric signal has a more regional character. The stratospheric pattern clearly is a measure of the strength of the polar stratospheric vortex with more than 80 % of the total variance being explained right over the North Pole. However there are only some regions over the Northern Hemisphere where more than 20% of the local variance of the 500 hPa field is explained. These regions are concentrated over the North Atlantic. The strongest signal appears over the North American archipelago, the Davis Strait and Greenland, where up to 70 % of the total variance is explained. Smaller spots with up to 30 % of explained variance occur over the mid-latitudes in the western North Atlantic, over Western Europe and in the far eastern Asia.

The first pair of associated canonical patterns describes a relationship between the stratospheric and the tropospheric circulation that was already found with simple linear model studies (e.g. Grieger and Schmitz, 1984). An anomalously intensive cyclonic vortex in the lower stratosphere is connected with a change of the tropospheric circulation over the whole North Atlantic (positive time coefficients of the canonical variables). The trough normally occurring downwind of the Rocky Mountains is strengthened and shifted somewhat to the east. Thus, over the western North Atlantic a more zonal circulation develops, and over the eastern North Atlantic a south westerly component of the tropospheric circulation is enhanced. In general the associated patterns of the first canonical mode of geopotential anomalies are similar throughout the troposphere. In Figure 9 the tropospheric part of the associated patterns and its pattern of explained local variances of the first canonical mode of the CCA of the 50 hPa and the 850 hPa geopotential fields are shown. The Greenland trough is associated with some baroclinic effects, leading to a westward shift of the trough axis with the height. While the trough is centred over East Greenland in the lower troposphere, it lies over the Davis Strait in the upper troposphere. This circulation anomaly is then connected with temperature anomalies as described in Graf et al. (1993b).

With a strong stratospheric vortex a positive geopotential anomaly over East Asia is also observed. An anomalously weak stratospheric vortex on the other hand is connected with an anomalously weak North American trough, diminished westerly winds over the North Atlantic, and a negative tropospheric geopotential height anomaly over East Asia (negative time coefficients of the canonical variables).

A time series of the canonical variables giving the weights of the above

described anomaly patterns for the individual winter months is given in Figure 7 together with the sea surface temperature anomaly (SSTA) over the eastern tropical Pacific (Wright, 1989). The canonical variables for the troposphere and the stratosphere are correlated with r=0.70. In Figure 8a (b) the scatter diagram of the time series of the canonical variable of the 50 hPa (500 hPa) geopotential field and the SSTA is shown. The 0.5 standard deviations (stdv) are indicated by shading, the asterisks and squares denote El Niño months and Volcano months, respectively. The numbers in the scatter diagram express the fourfold table (or 2x2 table) for the canonical variables versus the SSTA, provided that only anomalies exceeding 0.5 stdv ("physically meaningful anomalies") are included in the analyses. The χ^2-tests for both fourfold tables show that the hypothesis of independence of SSTA anomalies and the canonical variables is refused at a confidence level of 99%. An exclusion of the volcanically disturbed years (i.e. 1963/64 after Agung; 1982/83 after El Chichón, indicated by open squares in the Figure 8) reduces the scatter somewhat. The connection between the SSTA in the eastern equatorial Pacific and the strength of the polar night vortex was already suggested by Labitzke and van Loon (1987). If only the El Niño years are considered that are not volcanically disturbed, 12 (6) out of the 18 winter months have a weakened (strengthened) polar night vortex. In this case a zonal wave number one disturbance is enhanced (see Figure 13 and the text below). Then the mean anomaly of all 18 months gives the weaker than normal polar night vortex described in Labitzke and van Loon (1987). Again selecting only the not volcanically disturbed winter months of El Niño years of the tropospheric time series of the canonical variable (Figure 8b), a preference for negative values of the weight of the tropospheric associated pattern of the first mode of the CCA is obvious (12 negative versus 6 positive weights).

The second canonical mode, characterized by essentially the same value (r=0.68) of the canonical correlation coefficient as the first mode, is shown in Figure 10. The stratospheric canonical correlation pattern is characterized by a zonal wave number one, much like the second EOF (Figure 2b) with extremes over North America and West Siberia. At these places also the highest values of explained local variance appear (Figure 11). The tropospheric part of the associated patterns depicts a Pacific North America Oscillation (Wallace and Gutzler, 1981). These patterns do not show any horizontal shift throughout the troposphere. Obviously they depict a barotropic mode (see also the temperature analysis below). In the troposphere, there are no significant anomalies found over Eurasia. The tropospheric explained local variance in Figure 11 has the highest

value is in the Aleutian low area (> 50 %), the other two centres of suggestive values being over the central North Pacific and over the Great Plains.

Positive (negative) values of the canonical variable of the second mode mean that in the middle troposphere a weak (strong) Aleutian low is flanked by negative (positive) geopotential height anomalies over the central North Pacific and over large parts of North America (Figure 12).

For the second mode there exist correlations, which are significantly different from zero at the 95% confidence level, for the stratospheric (r=-0.33) and for the tropospheric (r=-0.40) canonical variables with SSTA (Figure 12) even without selection of 'physically meaningful anomalies'. Again, the fourfold table (Figure 13) while proving a statistically significant correlation, gives evidence of the considerable scatter. In the case of El Niños (excluding those accompanied by strong explosive volcanic eruptions) 12 (13) out of the 18 winter months have positive weights of the stratospheric (tropospheric) canonical variable, i.e. are associated with a deep trough over central North America.

As can easily be determined from the scatter diagrams, both canonical modes can have high loading even without any known external forcing (Volcanos and El Niño, open squares and asterisks, respectively, in Figure 8 and Figure 13). Therefore we call them natural associated modes.

4.3.2. Temperature

In terms of climate variability, the temperature of the lower troposphere is the most interesting parameter to the public. Thus, we also performed an analysis of the canonical correlation between the stratospheric circulation and tropospheric temperatures of the 850 hPa.

The first canonical mode (canonical correlation of 0.71) of the associated patterns of the 50 hPa geopotential height anomalies (Figure 14) and the lower tropospheric air temperature corresponds to the second mode of the geopotential CCA from chapter 4.3.1. The stratospheric canonical correlation pattern is again very similar to the second EOF (Figure 2b). The difference from the geopotential CCA is a deeper North American low and a flatter high over eastern Siberia in the stratosphere. As can be seen from Figure 15b, the area with substantially explained variance of the tropospheric temperature is mainly the central part of

North America north of 40°N, where up to 50% of local variance is explained. Two further areas with suggestive values of explained variance are situated in the Northeast Pacific and over East Siberia. The main feature of the association of stratospheric geopotential and lower tropospheric temperature is the North America anomaly. This feature obviously is a barotropic phenomenon. It can be traced throughout the whole troposphere (not shown here) without any local shifts between temperature and geopotential anomaly patterns.

The second canonical mode (canonical correlation coefficient r=0.64) of the tropospheric temperature analysis (associated patterns Figure 16) is similar to the patterns Graf et al. (1993b) found with a simple selection of strong and weak polar winter vortexes. The stratospheric canonical correlation pattern corresponds to the first EOF. In the tropospheric temperature field most of the local variance can be explained over the North Atlantic and adjacent continental areas. The highest values (50%) are found over the Davis Strait and over the North Sea and western Scandinavia (Figure 17). The associated patterns suggest positive (negative) lower tropospheric temperature anomalies in case of a strong (weak) polar winter vortex over northern Eurasia and cold (warm) conditions over Northwest America to Greenland. As was outlined previously (Graf et al., 1993b) these temperature anomalies are mainly due to advective processes. The baroclinicity associated with these processes can be seen from a comparison of Figure 9a (geopotential anomalies) and Figure 16b (temperature anomalies).

4.4. Local studies

An estimation of the significance of the canonical modes found proves to be difficult. However, in our investigation the stratospheric canonical variable essentially follows the stratospheric EOFs used. Therefore, the correlation between the PCs and the time series of the tropospheric fields can be calculated. In Figure 18a (b) the patterns of correlation coefficients between the first PC of the 50 hPa Geopotential and the original, unfiltered time series of the 500 hPa geopotential (850 hPa temperature) and in Figure 19a (b) the same for the second PC are shown. A correlation coefficient of 0.33 (0.37) is significantly different from zero at the 95% confidence level for 32 (27) realizations in time. It becomes clear, that the correlation patterns follow the optimized results of the CCA (Figures 5b, 10b, 14b and 16b respectively). As was to be expected, the explained variance in the raw data fields is smaller than in the EOF filtered data.

5. Conclusions

Applying the Canonical Correlation Analysis technique to stratospheric geopotential and tropospheric geopotential fields and the 850 hPa temperature field of the northern hemisphere for a 32 year (1957/58-1988/89; 500 hPa geopotential) or a 27 year (1962/63-1988/89; 200 hPa, 700 hPa, 850 hPa geopotential, 850 hPa temperature) period of winter months, two natural modes were found. These modes associate geopotential anomalies in the northern hemisphere winter stratosphere with circulation and temperature anomalies in the troposphere. The method applied does not allow any statements about cause and effect. The order of the modes is determined by the canonical correlation coefficient (CCC). Both modes have comparable CCCs. A more distinct difference was found in the vertical structure of the tropospheric part of the mode. Here we found one mode which is more baroclinically influenced in the troposphere. This mode is associated with the strength of the polar winter vortex in the stratosphere. The mode describing a zonal wave number one in the stratosphere is associated with barotropic features in the troposphere. In the troposphere this barotropic mode shows a pattern much like the PNA. The investigation of the canonical variables showed a connection between the strength of the barotropic mode and El Niño events. During El Niños a strengthened Aleutian low and a positive geopotential anomaly over North America (positive PNA-Index) are connected with a zonal wave number one structure in the stratosphere with a ridge over North America and a trough over East Asia. Model experiments with prescribed SSTA of the El Niño type (Kirchner and Graf, 1993) showed that this natural mode may be driven by the tropospheric anomalies. The baroclinic mode, however was enhanced in model studies (Boville, 1984; Kodera et al., 1991; Graf et al., 1993b) from the stratosphere. This mode is determined by a strong polar night vortex in the stratosphere, which besides natural variability can be forced by low latitude volcanic aerosols. The strongest tropospheric effects in this case are found over the North Atlantic in the geopotential field with strengthened westerlies leading to positive temperature anomalies over northern Eurasia. The strong negative temperature anomalies in the east of North America are due to the advection of polar air at the windward side of the Greenland trough.

Kodera (1993c) discussed the effect of the cooling trend of the polar stratosphere in winter on the tropospheric circulation. Based on our geopotential trend analysis for the lower stratosphere, we suggest that an indirect greenhouse effect is responsible for the polar cooling. The increase of tropospheric temperature in lower latitudes due to combined greenhouse gas effects leads to an initial intensi-

fication of the polar winter vortex. The intensified vortex then causes polar cooling which in a positive feedback loop is still strengthened. The dynamic coupling between stratospheric and tropospheric winter circulation, described by our baroclinic mode, is then responsible for positive temperature anomalies over the continents in northern middle and high latitudes (Graf et al., 1993b). We investigated whether this chain of effects also works in the GCM (ECHAM3-T42) experiments, performed by Perlwitz et al. (1994) to study the 3xCO2 greenhouse effect. We found that, though the northern polar stratosphere cools down slightly, the polar vortex is not increased as much as would be needed to cause the above mentioned coupling mechanism. The main shortcoming of the GCM is the inadequate variability of the polar night vortex. Therefore the dynamic effects of the coupling between stratospheric and tropospheric circulation are not included correctly. The temperature effects found in the model's troposphere and stratosphere are solely due to the equally distributed greenhouse gases, i.e. tropospheric warming by increased long wave counter radiation is accompanied by a compensating stratospheric cooling. We speculate that this simple effect in the real world is dominated by dynamic effects during winter in the northern hemisphere. For further investigation a much better resolution of the stratospheric processes is needed in the models.

Acknowledgments

We wish to express our sincere thanks to the Stratospheric Research Group of Prof. Karin Labitzke from the Free University of Berlin, who supplied the data to us. Thanks are also due to Dr. G. Schmitz and V. Kharin for their interest and valuable discussion. This work in part was sponsored by contract No. 07-KFT-86/2 by the Bundesministerium für Forschung und Technologie.

References

Anderson, C. W., 1984: An introduction to multivariate statistical analysis. Wiley & Sons, 2nd edition, 675 p.

Barnett, T. P. and R. Preisendorfer, 1987: Origins and levels of monthly and seasonal forecast skill for United States surface air temperatures determined by canonical correlation analysis. Mon. Wea. Rev., 115, 1825-1850.

Barnston, A. G. and C. F. Ropelewski, 1992: Prediction of ENSO episodes using canonical correlation analysis. J. Climate, 5, 1316-1345.

Bretherton, C. S., C. Smith and J. M. Wallace, 1992: An intercomparison of methods for finding coupled patterns in climate data. J. Climate, 5, 541-560.

Boville, B. A., 1984: The influence of the polar night jet on the tropospheric circulation in a GCM. J. Atmos. Sci., 41, 1132-1142.

Charney, J. G. and P. G. Drazin, 1961: Propagation of planetary-scale disturbances from the lower into the upper atmosphere. J. Geophys. Res., 66, 83-109.

Déqué, M. and J. Servain, 1989: Teleconnections between tropical Atlantic sea-surface temperatures and mid-latitude 50-kPa heights during the period 1964-86. J. Climate, 2, 929-944.

Fraedrich, K., 1986: Estimating the dimensions of weather and climate attractors. J. Atmos. Sci., 43, 419-432.

Geller, M. A. and J. C. Alpert, 1980: Planetary wave coupling between the troposphere and the middle atmosphere as a possible sun-weather mechanism. J. Atmos. Sci., 37, 1197-1215.

Glahn, H. R., 1968: Canonical correlation analysis and its relationship to discriminant analysis and multiple regression. J. Atmos. Sci., 25, 23-31.

Graf, H.-F., I. Kirchner, A. Robock and I. Schult, 1993a: Pinatubo eruption winter climate effects: model versus observations. Climate Dynamics, 9, 81-93.

Graf, H.-F. and J. Perlwitz, 1994: On the long term behaviour of the stratospheric and tropospheric circulation parameters. (in prep.)

Graf, H.-F., J. Perlwitz and I. Kirchner, 1993b: Northern hemisphere tropospheric mid-latitude circulation after violent volcanic eruptions. MPI Report, 107, 18 pp.,(also: Contr. Phys. Atmos., 67, 1994).

Graham, N. E., J. Michaelsen and T. P. Barnett, 1987: An investigation of the El Niño-Southern Oscillation cycle with statistical models. 1. Predictor field characteristics. J. Geophys. Res., 92, 14251-14270.

Grieger, N. and G. Schmitz, 1984: The northern hemisphere stationary planetary waves and associated Eliassen-Palm cross-sections of the stratosphere and mesosphere, Z. Meteor., 34, 341-353.

Groisman, P. Y., 1992: Possible regional climate consequences of the Pinatubo eruption: An empirical approach. Geophys. Res. Lett., 19, 1603-1606.

Hines, C. O., 1974: A possible mechanism for the production of sun-weather correlation. J. Atmos. Sci., 31, 589-591.

Hotelling, H., 1936: Relations between two sets of variates. Biometrika, 28, 321-377.

Kirchner, I. and H.-F. Graf, 1993: Volcanos and El Niño-signal separation in winter. MPI Report, 107, 57pp.

Kodera, K., 1993a: Influence of the stratospheric circulation change on the troposphere in the northern hemisphere winter. In: M.-L. Chanin (ed.): The role of the stratosphere in global change. pp. 227-243, Springer Verlag, Berlin.

Kodera, K., 1993b: Influence of volcanic eruptions on the troposphere trough stratospheric dynamical processes in the northern hemisphere winter, J. Geophys. Res., in press.

Kodera, K., 1993c: A possible influence of recent polar stratospheric coolings on the troposphere in the northern hemisphere winter. (submitted to J. Geopshys. Res.)

Kodera, K. and K. Yamazaki, 1990: Long-term variation of upper stratospheric circulation in the northern hemisphere in December. J. Meteorol. Soc. Japan, 68, 101-105.

Kodera, K., M. Chiba, K. Yamazaki and K. Shibata, 1991: A possible influence of the polar night jet on the subtropical tropospheric jet. J. Meteorol. Soc. Japan, 69, 715-721.

Labitzke, K. and H. van Loon, 1987: The Southern Oscillation. Part V: The anomalies in the lower stratosphere of the northern hemisphere in winter and a comparison with the Quasi-Biennial Oscillation. Mon. Wea. Rev.,115, 357-369.

Labitzke, K. and H. van Loon, 1988: Association between the 11-year solar cycle, the QBO, and the atmosphere. Part I: the troposphere and the stratosphere in the northern hemisphere in winter. J. Atm. Terr. Phys., 50, 197-206.

Labitzke, K. and H. van Loon, 1991: Some complications in determined trends in the stratosphere. Adv. Spac. Res., 11, 321-330.

Labitzke, K. and van Loon, 1994: A note on trends in the stratosphere: 1958-1992. COSPAR Colloquia Series, 5.

Matsuno, T., 1970: Vertical propagation of stationary planetary waves in the winter northern hemisphere. J. Atmos. Sci., 27, 871-883.

Metz, W., 1989: Low-frequency anomalies of atmospheric flow and the effects of cyclone-scale eddies: a canonical correlation analysis. J. Atmos. Sci., 46, 1026-1041.

North, G. R., T. L. Bell, R. F. Cahalan and F. J. Moeng, 1982: Sampling errors in the estimation of empirical orthogonal functions. Mon. Wea. Rev., 110, 699-706.

Perlwitz, Jan and U. Cubasch, 1994: Simulation of greenhouse warming with the ECHAM3 mode using the time-slice method. (in prep.)

Robock, A. and J. Mao, 1992: Winter warming from large volcanic eruptions. Geophys. Res. Lett., 12, 2405-2408.

Röhr, M., 1987: Canonical correlation analysis (German). Akademieverlag, Berlin, 181 pp.

Schmitz, G. and N. Grieger, 1980: Model calculations on the structure of planetary waves in the upper troposphere and lower stratosphere as a function of the wind field in the upper stratosphere. Tellus, 32, 207-214.

Wallace, J. M. and D. S. Gutzler, 1981: Teleconnections in the geopotential height field during the northern hemisphere winter. Mon. Wea. Rev., 109, 784-812.

Wallace, J. M., C. Smith and C. S. Bretherton, 1992: Singular value decomposition of wintertime sea surface temperature and 500-mb height anomalies. J. Climate, 5, 561-576.

Wright, P. B., 1991: Homogenised sea surface temperature from the COADS and sea surface temperature from Climate Diagnostic Bulletin of the Climate Analysis Centre.

Zorita, E., V. Kharin, and H. v. Storch, 1992: The atmospheric circulation and sea surface temperature in the North Atlantic area in winter; Their interaction and relevance for Iberian precipitation. J. Climate, 5, 1097-1108.

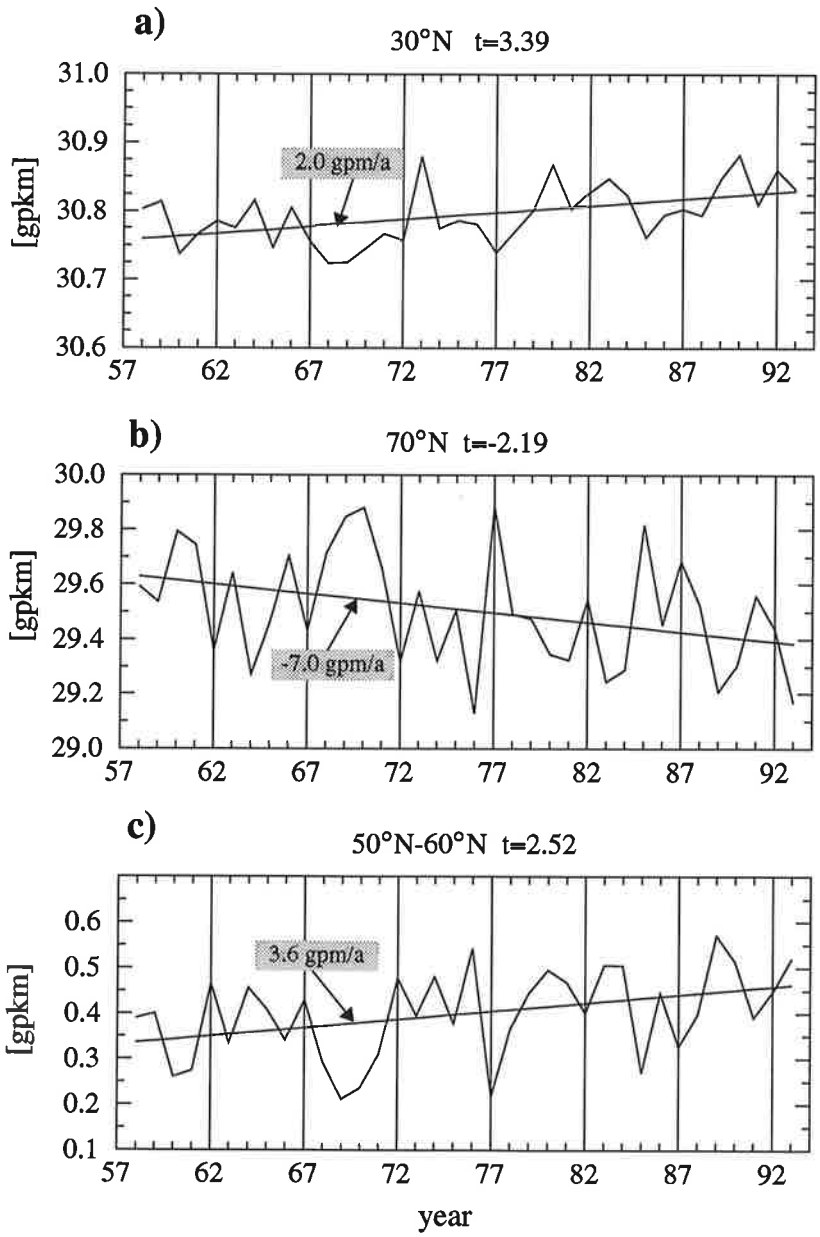

Figure 1:

Winter mean ($\overline{DJF}$) time series (57/58-92/93) of the zonally averaged 50 hPa geopotential height together with the linear trend function for 30°N (a) and 70°N (b), and the difference time series together with the linear trend function for 50°N-60°N (c) corresponding to the strength of polar night jet. (t: t-test value for the linear regression coefficient)

a)

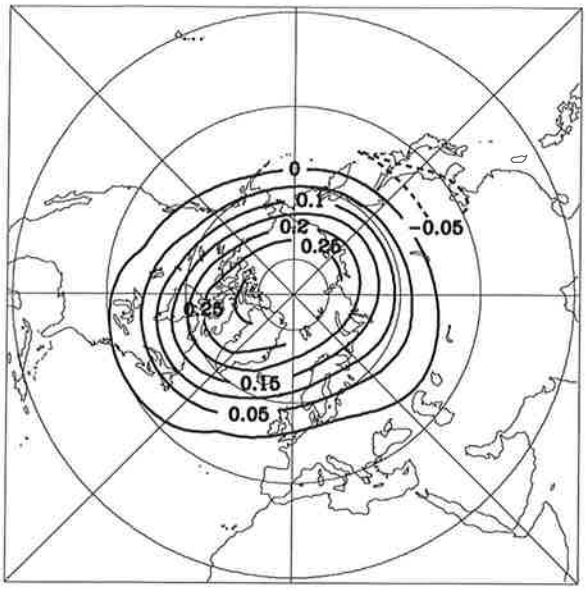

b)

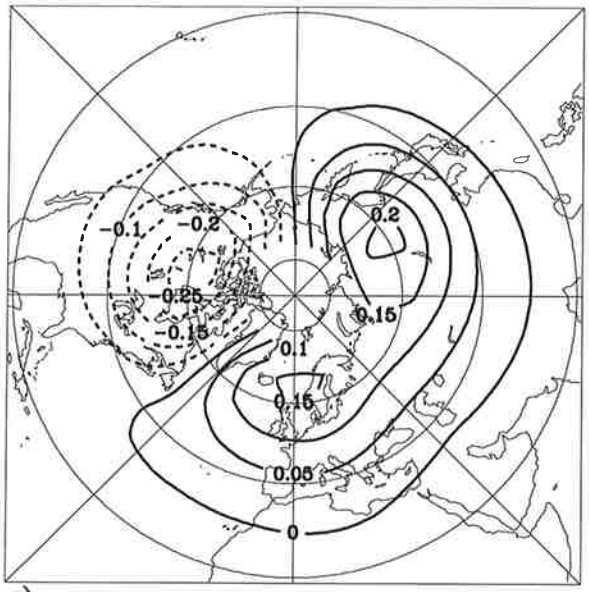

c)

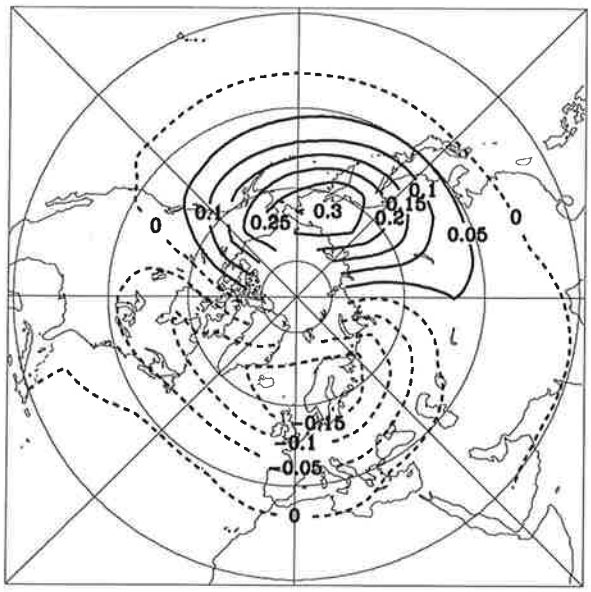

Figure 2:

First (a), second (b) and third (c) EOF of the monthly mean 50 hPa geopotential height, calculated for the winter months (DJF). They explain 52%, 14% and 8% of the total variance, respectively.

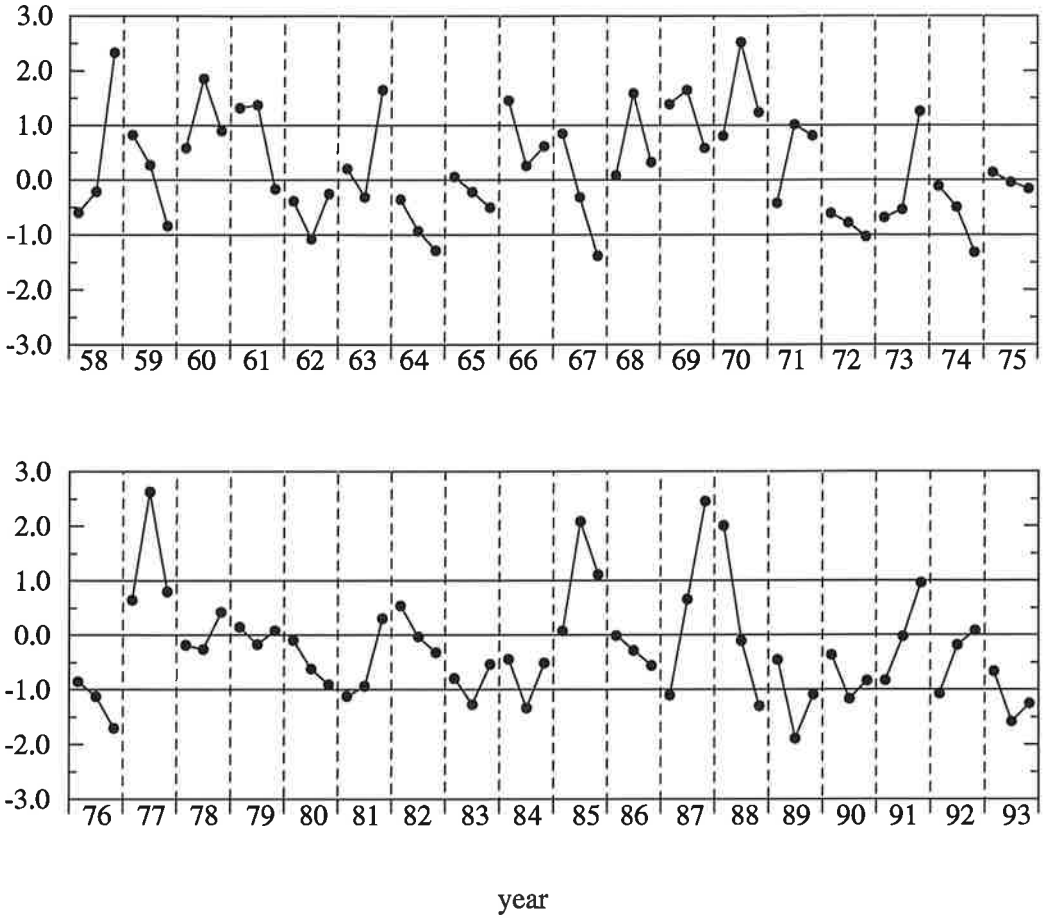

Figure 3:
First normalized principle component of the 50 hPa geopotential height (corresponding to Figure 2a)

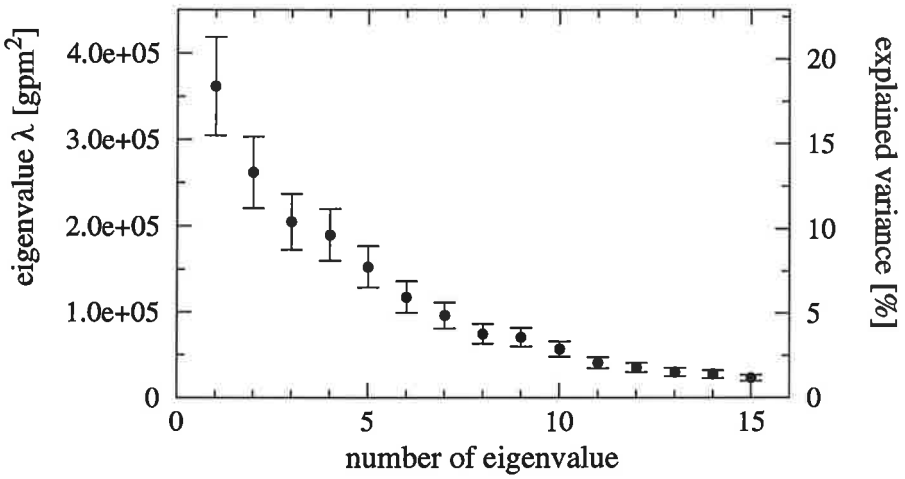

Figure 4:

First 15 eigenvalues λ of the 500 hPa geopotential height EOF-analysis (calculated for the in winter months DJF) with error bars representing an estimate of the standard error (one standard deviation $\delta\lambda \sim \lambda\sqrt{2/N}$ for N=96).

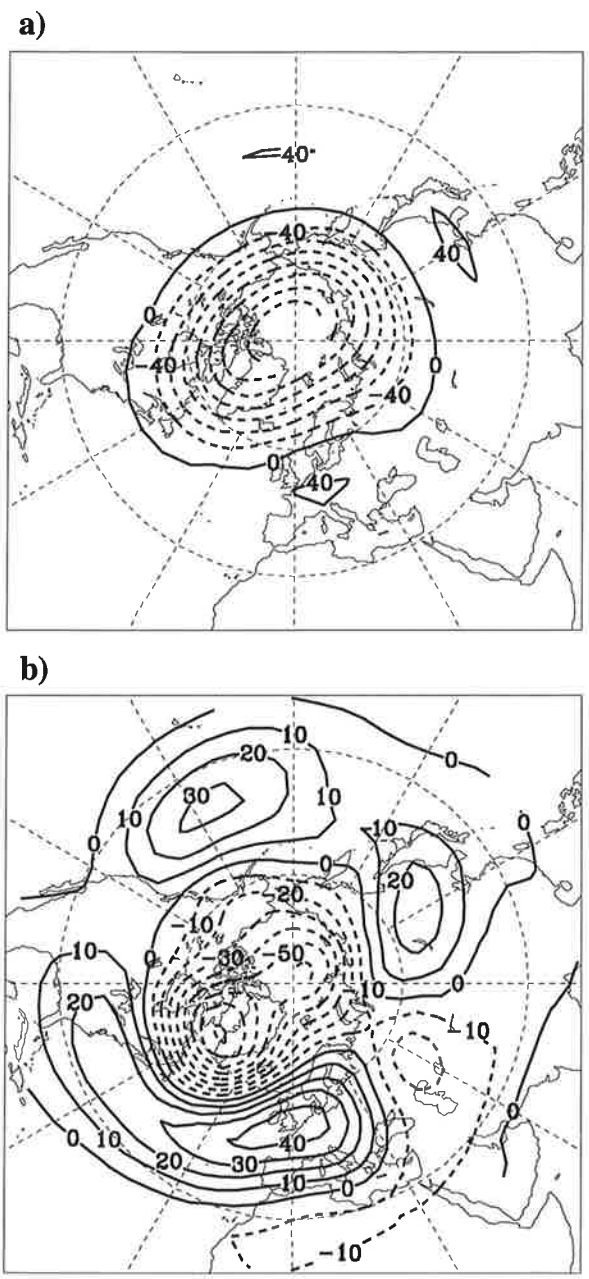

Figure 5:

Associated patterns of the first canonical mode of the 50 hPa geopotential field (a) contour interval: 40 gpm), and the 500 hPa geopotential field (b) contour interval: 10 gpm).

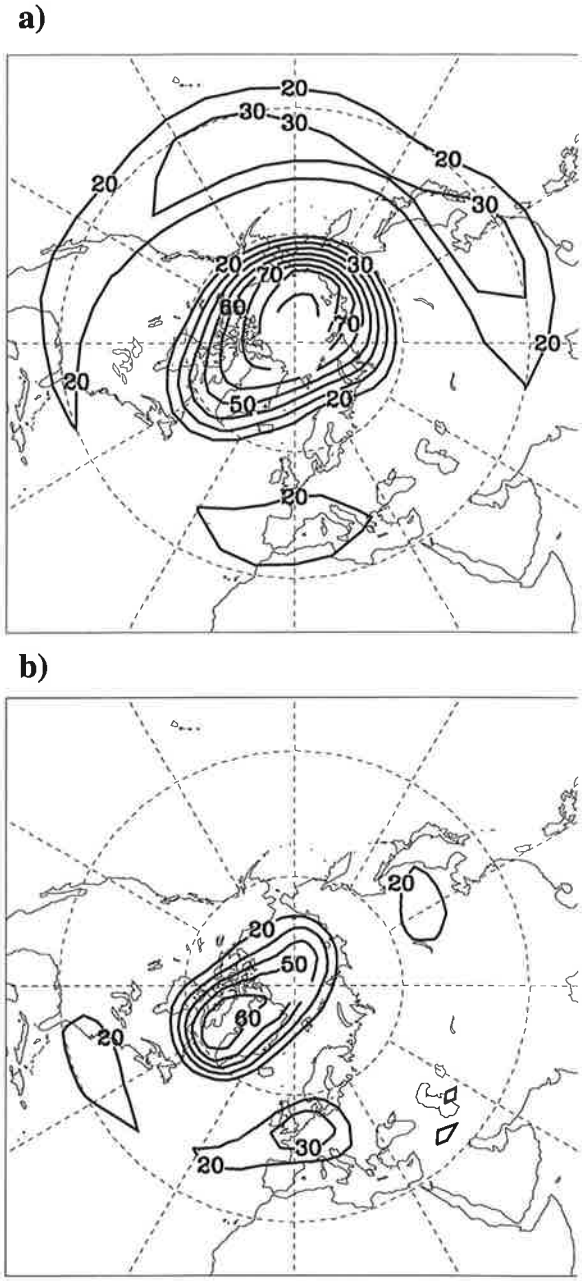

Figure 6:

Patterns of percent of local variance explained by the pair of the canonical variables of the first canonical mode in their corresponding original data fields (a) 50 hPa geopotential field, b) 500 hPa geopotential field)

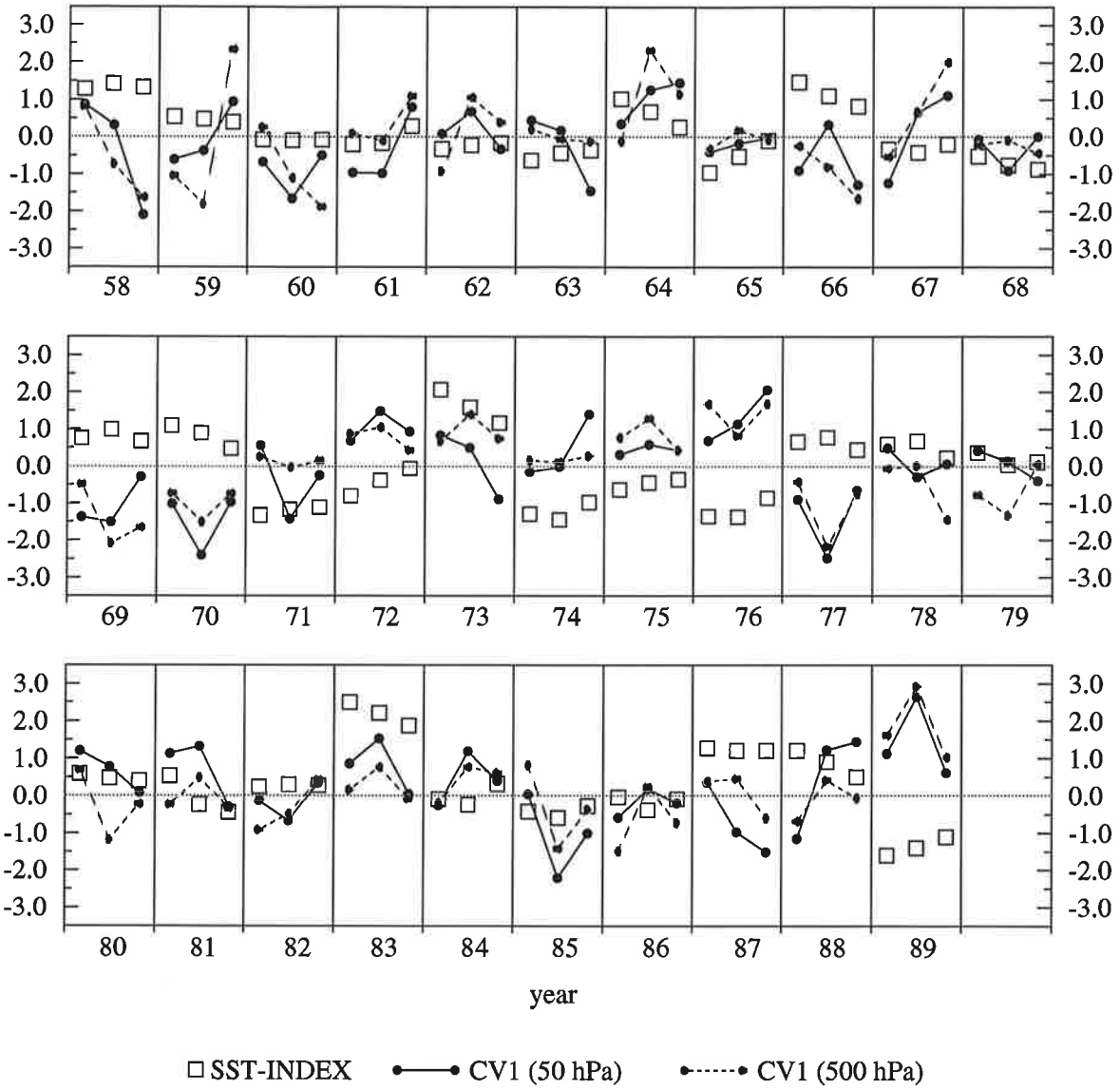

Figure 7:

Pair of canonical variables of the first canonical mode (CV1) of the CCA of the 50 hPa geopotential field (solid lines) and the 500 hPa geopotential field (dashed lines), and the tropical SST-Index (open squares). (The CCA is calculated only for the winter months DJF).

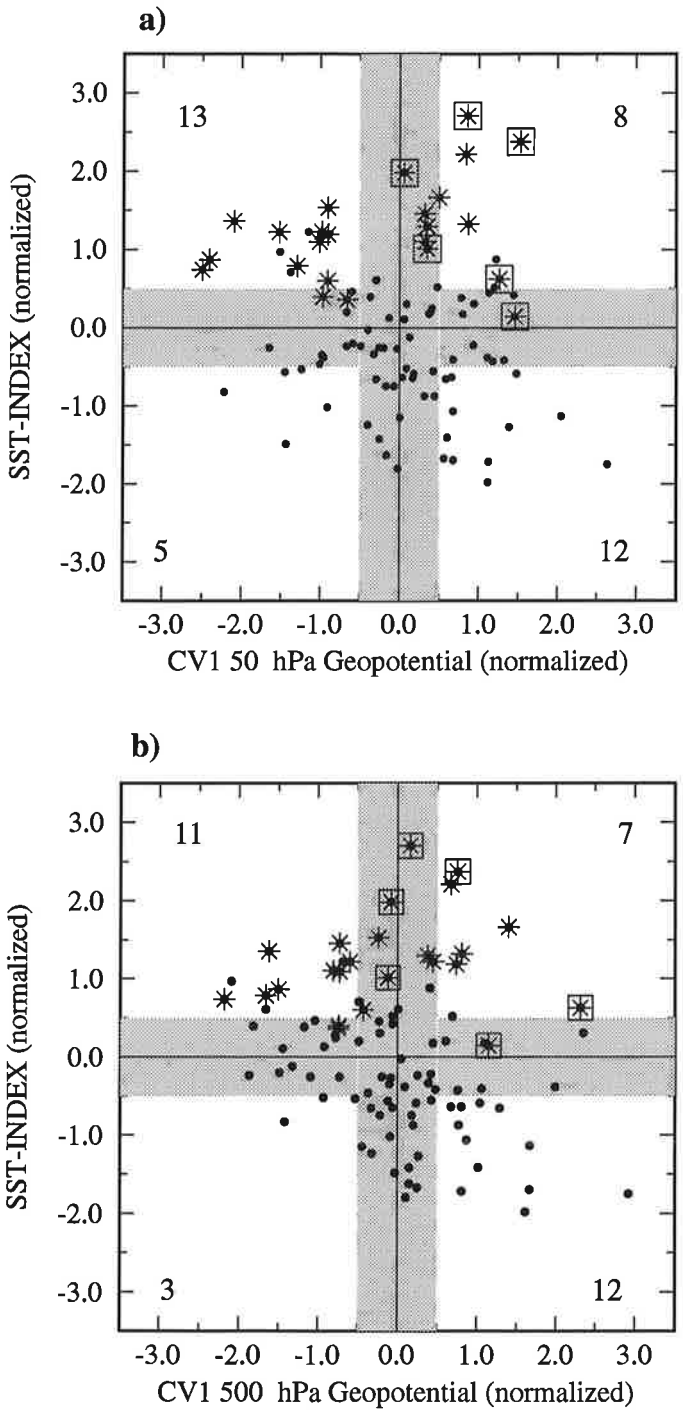

Figure 8:

a) Scatter diagram for canonical variable of the first mode (CV1) of the 50 hPa field and the SST-Index corresponding to Figure 7a. The asterisks (squares) are months with El Niño (Volcanos).0.5 stdv areas are indicated by shading.

b) The same for canonical variable of the first mode of the 500 hPa geopotential field and the SST-Index corresponding to Figure 7b.

a)

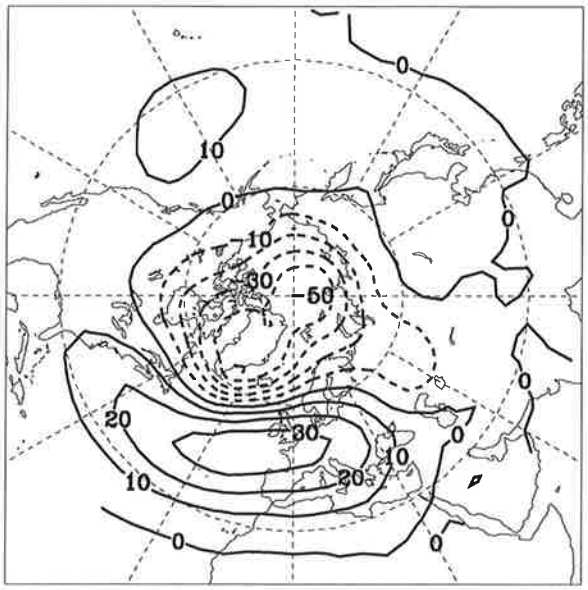

b)

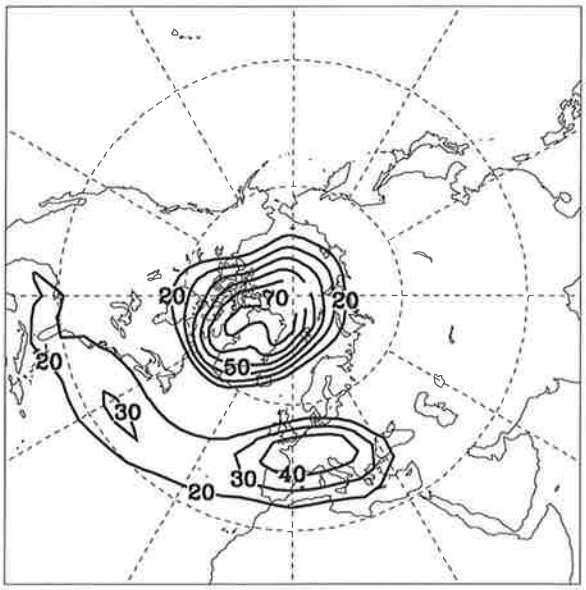

Figure 9:

a) Tropospheric part of the associated patterns of the first canonical mode of the CCA of the 50 hPa geopotential field and the 850 hPa geopotential field (contour interval: 10 gpm). and b) corresponding pattern of percent of local variance explained by their canonical variable .

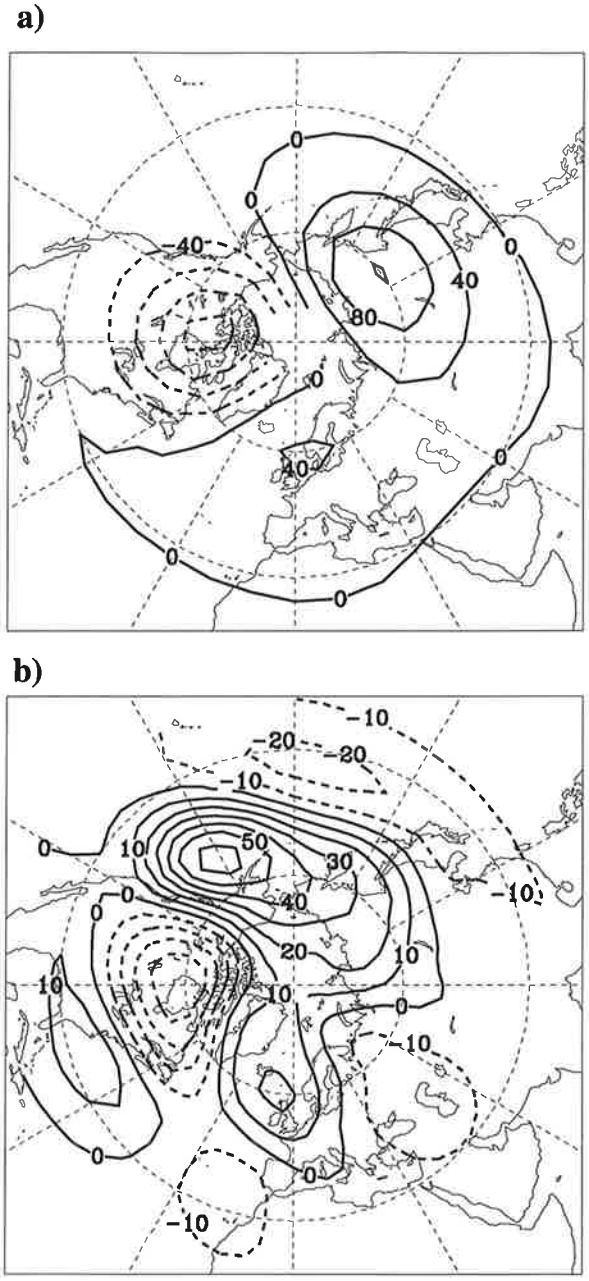

Figure 10:
As Figure 5, but for the second canonical mode.

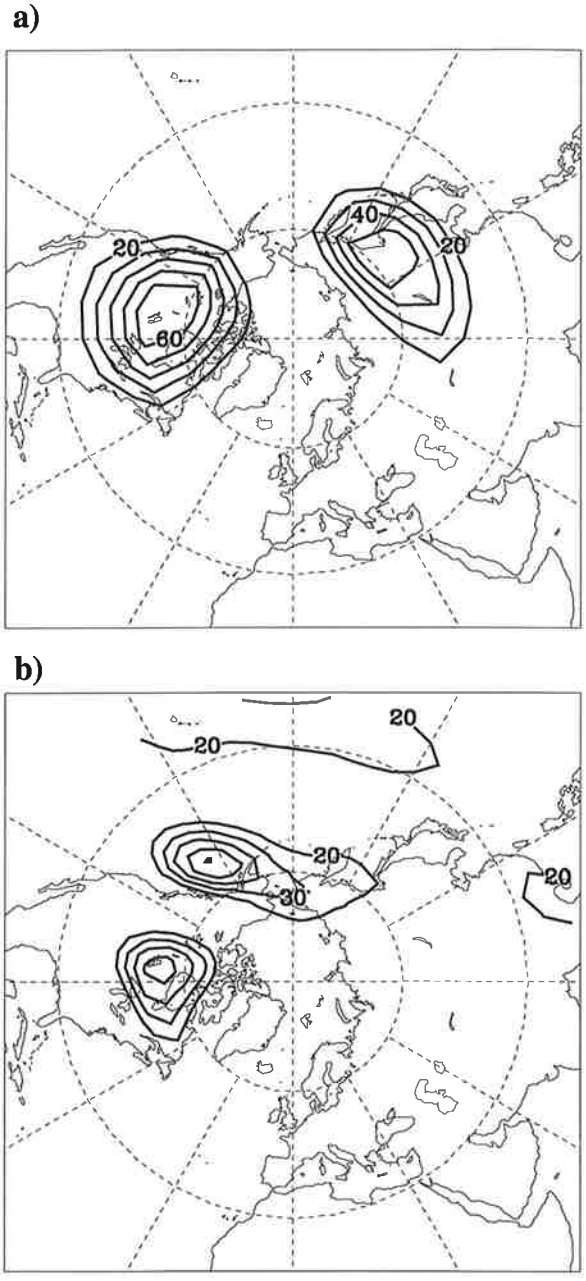

Figure 11:
As Figure 6, but for the second canonical mode.

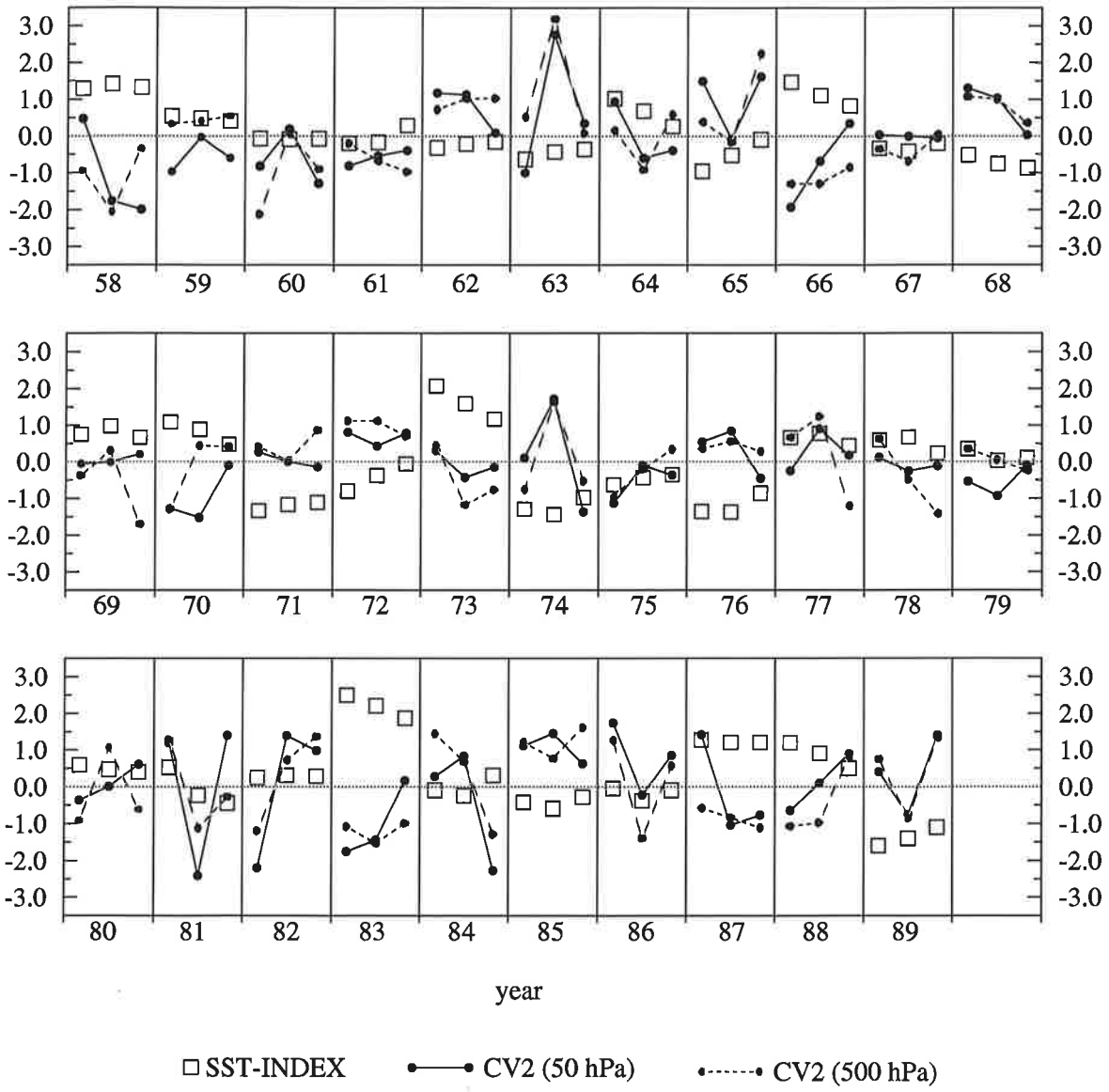

Figure 12:
As Figure 7, but for the second canonical mode.

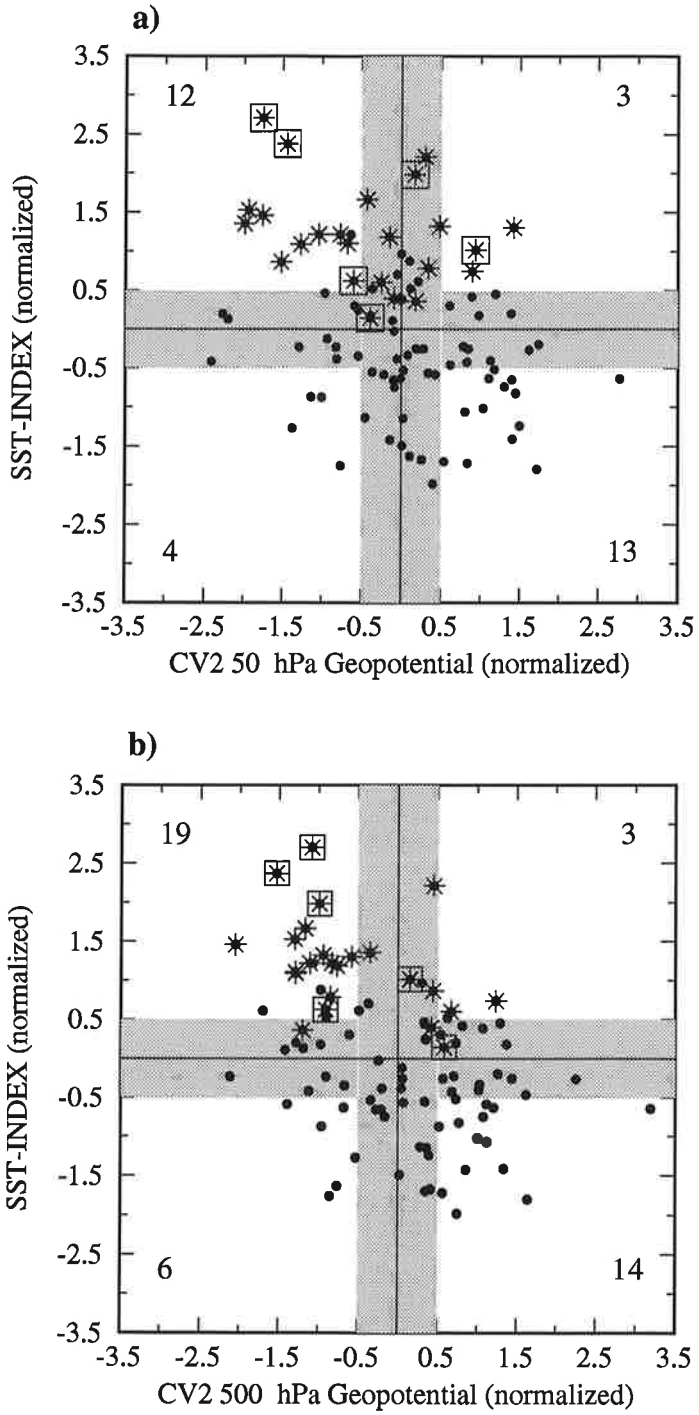

Figure 13:

a) Scatter diagram for canonical variable of the second mode of the 50 hPa field and the SST-Index corresponding to Figure 12a. The asterisks (squares) are months with El Niño (Volcanos). 0.5 stdv areas are indicated by shading.

b) The same for canonical variable of the second mode of the 500 hPa field and the SST-Index corresponding to Figure 12b.

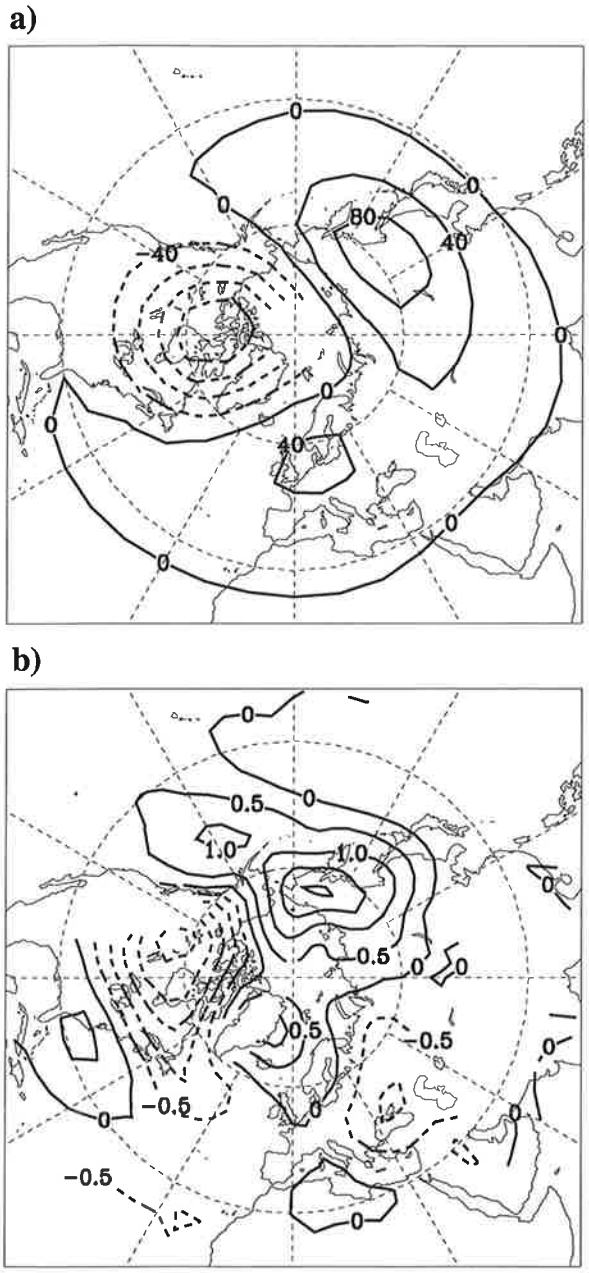

Figure 14:

Associated patterns of the first canonical mode of the 50 hPa geopotential field a), contour interval: 40 gpm); and 850 hPa temperature field b), contour interval: 0.5 K.

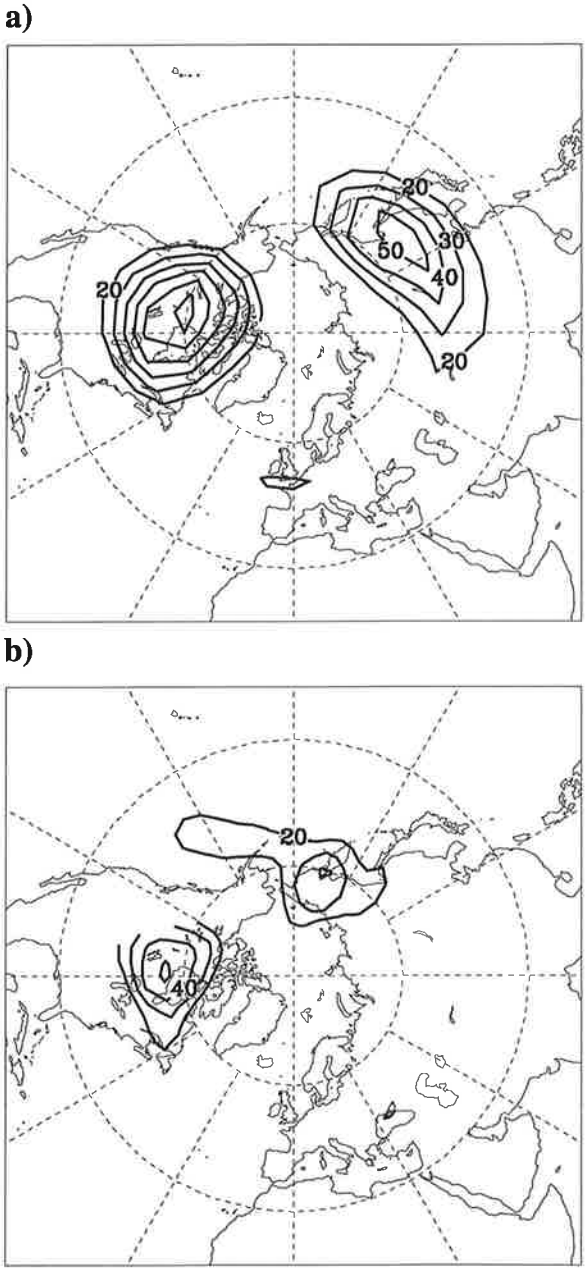

Figure 15:

Patterns of percent of local variance explained by the pair of canonical variables of the first canonical mode in thier corresponding original data fields (a) for 50 hPa geopotential field, b) for 850 hPa temperature field).

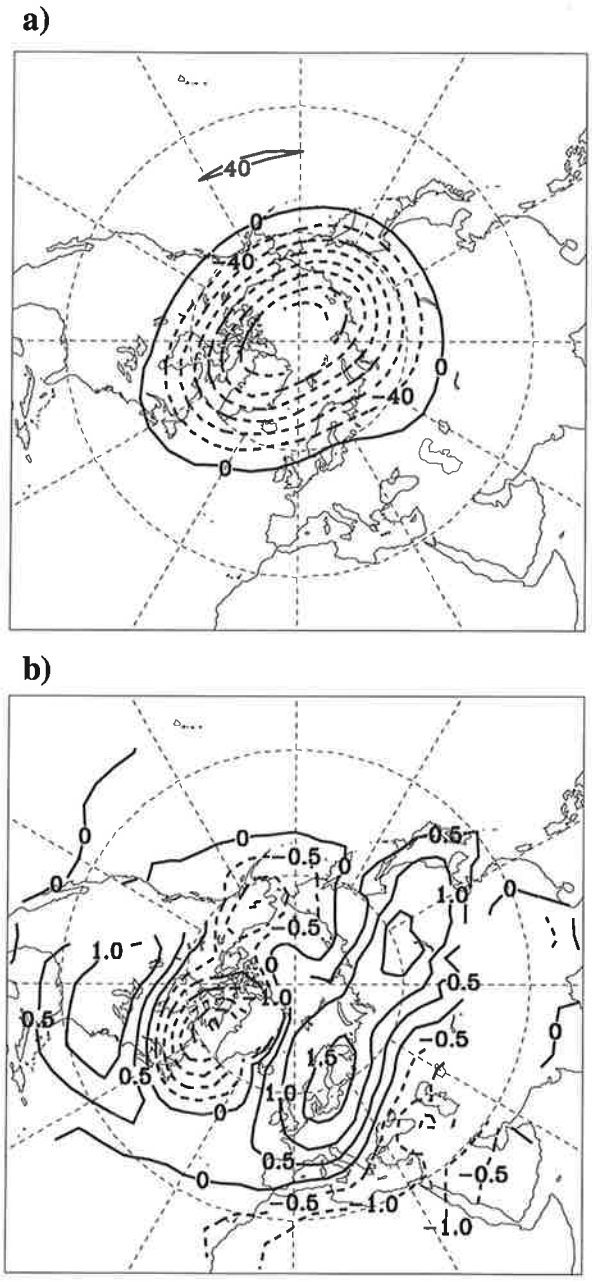

Figure 16:
As figure 14, but for the second canonical mode.

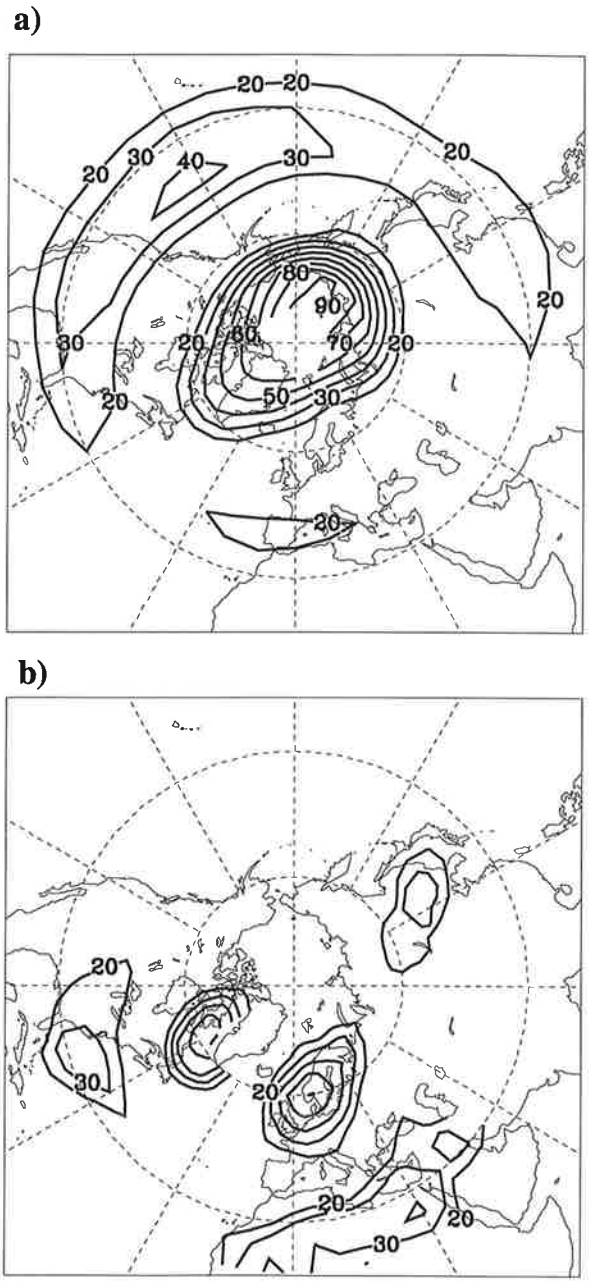

Figure 17:
As figure 15, but for the second canonical mode.

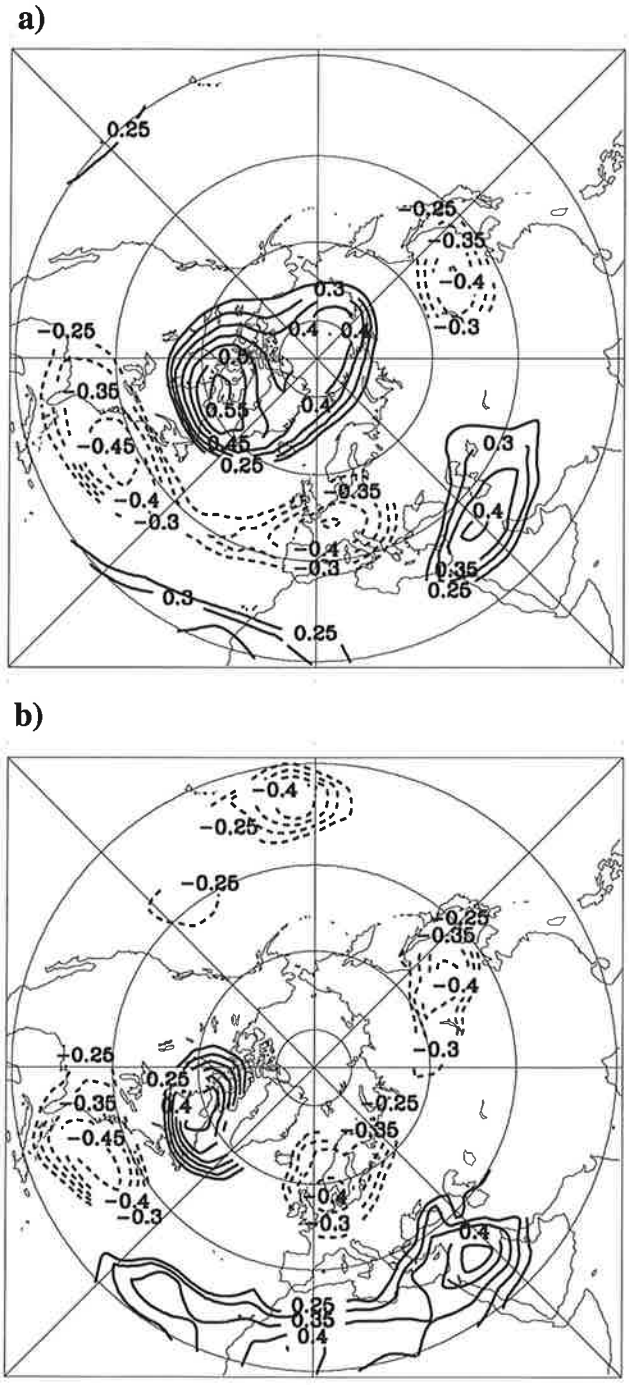

Figure 18:

a) Pattern of Correlation coefficients between first PC of the 50 hPa geopotential field and the time series of the 500 hPa geopotential field for the Winter months DJF (1957/58-1988/89).

b) Same like a, but for the temperature of the 850 hPa pressure level (1962/63-1988/89).

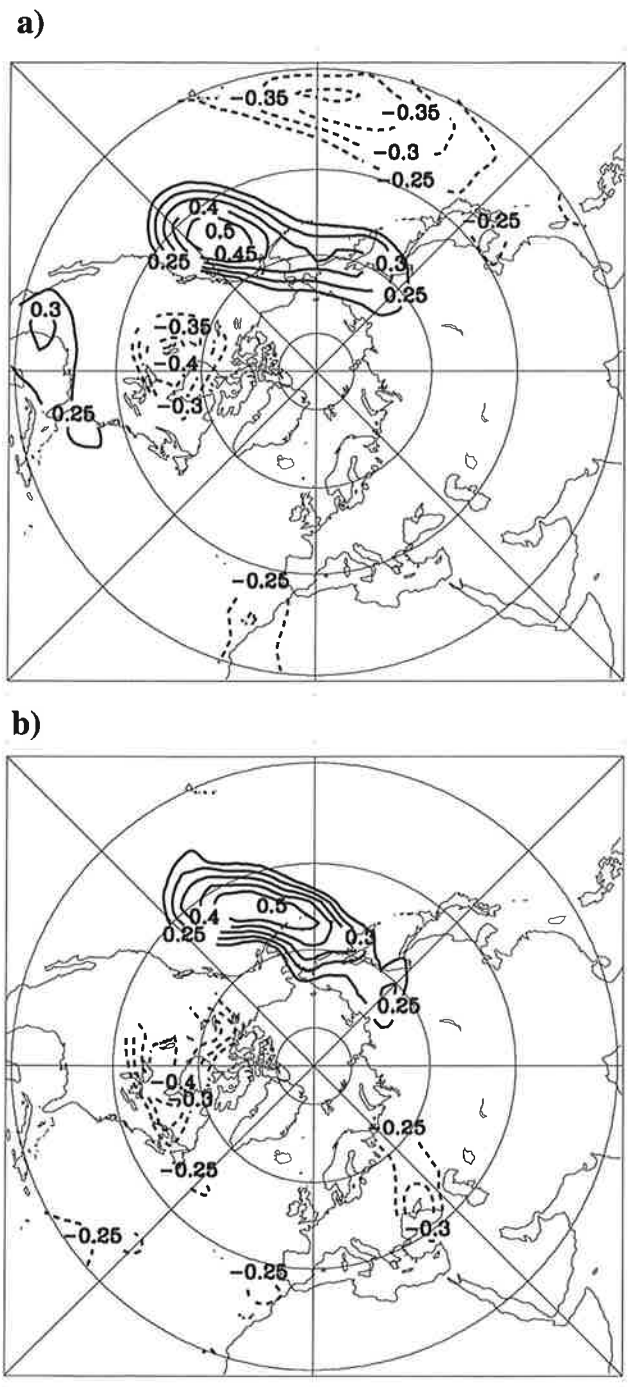

Figure 19:

a) Pattern of Correlation coefficients between second PC of the 50 hPa geopotential field and the time series of the 500 hPa geopotential field for the Winter months DJF (1957/58-1988/89).

b) Same like a, but for the temperature of the 850 hPa pressure level (1962/63-1988/89).